Magnetic behavior of the diluted magnetic semiconductor $Zn_{1-x}Mn_xSe$

A. Twardowski,* H. J. M. Swagten, and W. J. M. de Jonge
Department of Physics, Eindhoven University of Technology, NL-5600 MB Eindhoven, The Netherlands

M. Demianiuk
Institute of Technical Physics, Wojskowa Akademia Techniczna, Warsaw, Poland
(Received 26 March 1987)

The magnetic susceptibility and specific heat of the diluted magnetic semiconductor $Zn_{1-x}Mn_xSe$ have been measured in the temperature range 10 mK $< T <$ 40 K for $0.01 \leq x \leq 0.53$. A paramagnetic–spin-glass transition was observed in the whole concentration range. The concentration dependence of the freezing temperature T_f was found to be compatible with a radial dependence of the exchange interaction between manganese ions of the type $J(R) \sim R^{-6.8}$. Based on this observation, we calculated thermodynamic properties with the extended nearest-neighbor pair approximation. It appears that this approximation provides a good simultaneous description of the specific heat and high-field magnetization and reproduces Curie-Weiss temperature for parameters $J_0/k_B = -13$ K (nearest-neighbor interaction) and $J_i(R)/k_B = -7/R^{6.8}$ K (distant-neighbor interaction). A comparison is made with other dilute magnetic semiconductors, and the possible origin of the exchange mechanism is then discussed.

I. INTRODUCTION

During the past years extensive investigations have been performed on the magnetic behavior of diluted magnetic semiconductors (DMS's) (i.e., II-VI or II-V compounds containing controlled quantities of randomly substituted magnetic ions).[1] So far data have been obtained almost exclusively on systems of the type $A_{1-x}Mn_xB$, such as $Hg_{1-x}Mn_xTe$, $Cd_{1-x}Mn_xTe$, $Cd_{1-x}Mn_xSe$, $Zn_{1-x}Mn_xTe$, $(Cd_{1-x}Mn_x)_3As_2$, and $(Zn_{1-x}Mn_x)_3As_2$.[2,3] From these data, as far as available, a rather typical behavior is observed. This behavior can be characterized as follows.

(1) Curie-Weiss behavior of the magnetic susceptibility χ at high temperatures indicating antiferromagnetic (AF) Mn-Mn interactions.

(2) A cusp or kink in the low-temperature χ indicating a spin-glass-like transition at a temperature depending on the Mn concentration x.

(3) A magnetic contribution to the specific heat C_m with a broad maximum shifting to higher T with x.

(4) A field dependence of the magnetization M indicating AF interactions, usually accompanied with steps in high fields.

Originally this magnetic behavior was interpreted as arising from interactions between Mn ions situated at the nearest-neighbor (NN) sites in the host lattice.[4,5] This conjecture was strongly supported by the original observation of the spin-glass (SG) transition only *above* the percolation limit (x_c) of the host lattice.[4,5] It was suggested then that the SG transition was brought about by short-range [nearest-neighbor (NN)] AF interaction causing topological frustration effects due to the high symmetry of the host lattice. Recent results, however, for low Mn concentrations in $Hg_{1-x}Mn_xTe$,[1] $(Cd_{1-x}Mn_x)_3As_2$,[2] $(Zn_{1-x}Mn_x)_3As_2$,[3] $Cd_{1-x}Mn_xTe$,[6] $Cd_{1-x}Mn_xSe$,[7] and very recently $Zn_{1-x}Mn_xTe$ and $Zn_{1-x}Mn_xSe$,[8] reveal the existence of a SG phase also *below* x_c. The situation for $(Cd_{1-x}Mn_x)_3As_2$ is even more pronounced since in this case for $x > x_c$ the NN frustration mechanism is also excluded due to the simple-cubic symmetry of the host lattice.[2] Moreover, subsequent calculations on the basis of NN interactions only gave rise to a wide spread of exchange parameters deduced from various sets of data and the need to adjust the random distribution of the magnetic ions. To our knowledge no consistent set of parameters explaining all the data simultaneously has been obtained on this basis.

It is our claim that these discrepancies are mainly due to the fact that the long-range character of the interactions is not taken into account, as we have shown recently for $(Cd_{1-x}Mn_x)_3As_2$ (Ref. 2) and, though less extensive, for some other systems as well.[9] Moreover, as we argued before,[10] detailed knowledge about the range or radial dependence of this long-range interaction might yield valuable information about the driving physical mechanisms behind the Mn-Mn interaction in DMS's. In view of this we thought it worthwhile to study the magnetic properties of $Zn_{1-x}Mn_xSe$ in some detail. Preliminary results have been reported recently.[8] We will report susceptibility and specific-heat results in a wide composition range ($0.1 \leq x \leq 0.53$) and we will try to interpret these data (together with magnetization[11] data and high-temperature susceptibility[12]) simultaneously on the basis of one model incorporating short-range as well as long-range interaction in a random array.

II. EXPERIMENTAL RESULTS

The samples of $Zn_{1-x}Mn_xSe$ were grown by the modified Bridgman method under the pressure of a neu-

tral gas. The crystalline structure of this material was reported[13] to be cubic for $x \leq 0.06$, polytypic for $0.06 < x \leq 0.12$, and hexagonal for $x > 0.12$. In a previous magneto-optical investigation[14] of this material no essential influence of polytypism was found, although some scattering of energy gap for $x \geq 0.2$ was reported.[15]

The Mn concentrations x of the investigated samples as measured by microprobe analysis were 0.014 ± 0.001, 0.023 ± 0.002, 0.056 ± 0.002, 0.064 ± 0.006, 0.103 ± 0.005, 0.154 ± 0.004, 0.254 ± 0.003, and 0.53 ± 0.02. Generally these actual concentrations were considerably larger (typically 50%) than the nominal concentrations of the starting materials.

A. Low-temperature susceptibility

The ac susceptibility was measured with a conventional mutual inductance bridge operating in the region $100 < f < 2000$ Hz and fields less than 1 G. Some representative susceptibility data for various x are shown in Fig. 1. The results below 1.5 were obtained in a dilution refrigerator for which no adequate absolute calibration of χ was available, which may result in some deviation of the data at low temperatures. Figure 1 clearly shows an anomalous behavior of the susceptibility at a certain temperature T_f (freezing temperature) depending on the concentration of Mn ions (see Table I). The anomalies are cusplike for high concentrations and kinklike for low concentrations. A similar situation was reported for $(Cd_{1-x}Mn_x)Te$, where a well-pronounced cusp for $x > 0.3$ (Ref. 4) and a kink for $x < 0.15$ (Ref. 6) was observed. In contrast to the susceptibility, as we will see later on, no anomalous behavior can be detected in the specific heat.

dc susceptibility data, field-cooled as well as zero-field-cooled, are shown in Fig. 2 for concentrations above and below the percolation limit. This characteristic behavior supports the interpretation of the anomaly

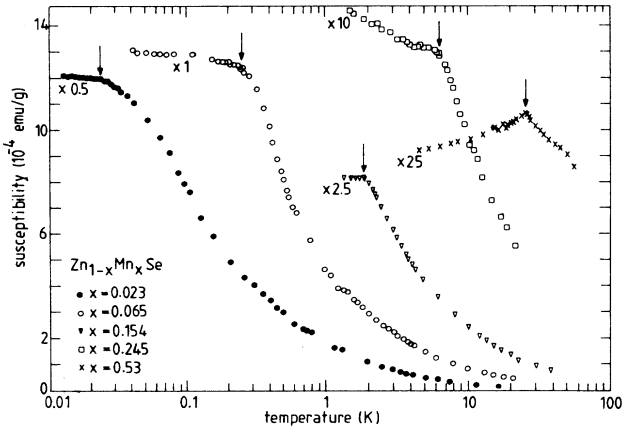

FIG. 1. ac susceptibility of $Zn_{1-x}Mn_xSe$ [$x = 0.023$ (●), 0.064 (○), 0.154 (▽), 0.245 (□), and 0.53 (×)] as a function of temperature for different Mn compositions. The arrows indicate the freezing temperatures T_f. Note the different vertical scales; the data are multiplied by the factor indicated in the figure.

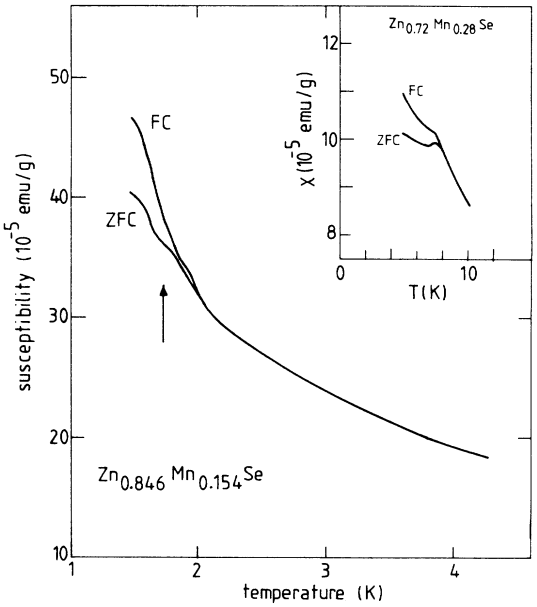

FIG. 2. dc susceptibility of $Zn_{0.846}Mn_{0.154}Se$ measured after zero-field cooling (ZFC, $H < 1$ G) and field cooling (FC, $H = 20$ G) as a function of temperature. The arrow indicates freezing temperature T_f as obtained from ac susceptibility. Inset: similar data for $Zn_{0.72}Mn_{0.28}Se$ (Ref. 12).

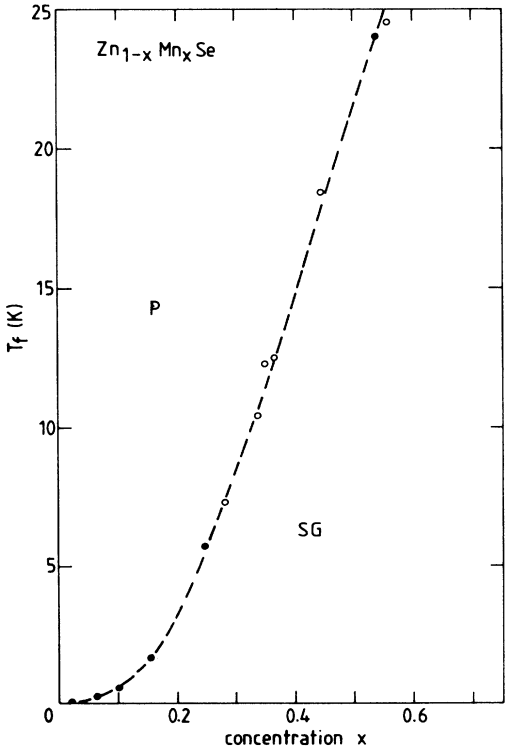

FIG. 3. Phase diagram for $Zn_{1-x}Mn_xSe$ (●, our data; ○, Ref. 12). The dashed line is a guide to the eye only.

TABLE I. Freezing temperatures T_f for $Zn_{1-x}Mn_xSe$.

T_f (K)	x
0.022	0.023
0.225	0.064
0.55	0.103
1.7	0.154
5.7	0.245
24	0.53

in the susceptibility as a transition to a spin-glass state. The resulting phase diagram, T_f-x, in the range $0.023 \leq x \leq 0.53$, is shown in Fig. 3. Inspection of this phase diagram shows that $T_f \rightarrow 0$ when $x \rightarrow 0$. From this experimental observation one may already conjecture that the interactions including this spin-glass transition are relatively long ranged, since otherwise no freezing should have been observed for x below the percolation limit, which amounts to $x_c = 0.18$ in this case.

B. Specific heat

Specific-heat data were obtained with a conventional adiabatic heat-pulse calorimeter in the temperature range $0.4 < T < 20$ K. The magnetic contribution C_m to the specific heat was obtained by subtraction of the lattice contribution of pure ZnSe and the nuclear hyperfine contribution of the Mn ions.

The results for C_m in zero external magnetic field are shown in Fig. 4. As quoted above, no anomaly was observed at the temperature T_f, indicated by arrows in the figure. The overall behavior of C_m is similar to that observed for the other DMS's: a broad maximum shifting to higher temperatures with increasing x. In our case

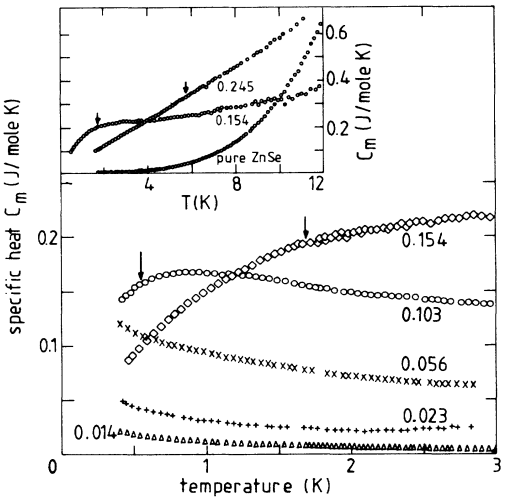

FIG. 4. Magnetic specific heat of $Zn_{1-x}Mn_xSe$ [$x=0.014$ (△), 0.023 (+), 0.056 (x), 0.103 (○), and 0.154 (◇)]. Inset: magnetic specific heat of $Zn_{1-x}Mn_xSe$ ($x=0.154$ and 0.245 as well as specific heat of pure ZnSe). The arrows indicate the freezing temperatures T_f.

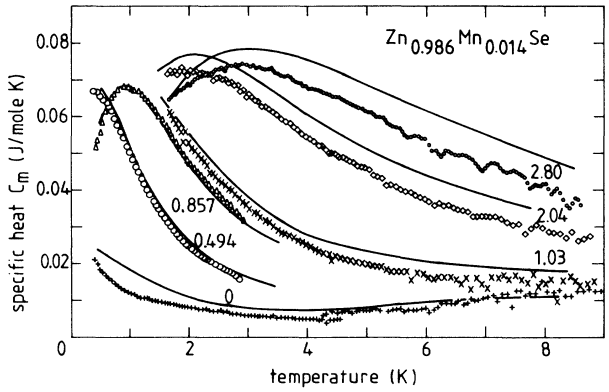

FIG. 5. Magnetic field dependence of the magnetic specific heat of $Zn_{0.986}Mn_{0.014}Se$ for $B = 0.00$, 0.494, 0.857, 1.03, 2.04, and 2.80 T. The solid lines are obtained from the ENNPA using $J_0/k_B = -13$ K and $J_i/k_B = -7/R^{6.8}$ K.

this maximum is not observed for $x \leq 0.06$ since it is located at temperatures lower than 0.4 K. In the presence of a magnetic field the specific-heat data show a shift of the maximum to higher temperatures with increasing field, as shown in Fig. 5 for $Zn_{0.986}Mn_{0.014}Se$. These data look very similar to earlier results[16] in the temperature range $0.3 < T < 3.5$ K on $Zn_{1-x}Mn_xSe$ with a *nominal* Mn concentration of 0.01. Quantitative comparison is, however, difficult since the actual Mn concentration is not known.

C. High-temperature susceptibility and magnetization

The magnetization has been measured up to 15 kOe and was reported earlier by one of the present authors.[11] For comparison some selected result will be shown later on. The high-temperature susceptibility results[12] show a Curie-Weiss behavior with $\Theta = -45$ K for $x = 0.05$ at high temperatures, indicating AF interactions between the Mn^{2+} ions. Moreover, Θ was found to be a linear function of the concentration[12] suggesting a random distribution of the Mn^{2+} ions.

III. INTERPRETATION

A. The spin-glass transition

Among the data reported above, the existence of a spin-glass transition for vanishingly small concentrations of x is the most obvious indication of the existence of long-range interactions between the Mn^{2+} ions.

As a basis for the interpretation we would like to focus our attention on this freezing transition since the concentration dependence of this transition can be considered as a probe of the radial dependence of the interaction strength between the impurities.[10]

In this respect it is relevant to note that the experimental data on the transition strongly support the spin-glass nature of the transition. These data include the cusp or kink in the ac susceptibility, the continuous be-

havior of the specific heat, and the hysterises observed in the dc susceptibility. These observations match perfectly the phenomenological characteristics which are commonly applied to define a transition to a canonical spin glass.[17]

If one accepts the nature of the transition as a spin-glass freezing (which is, however, disputed as we will argue in the discussion), then a scaling analysis should be applicable. Such a scaling analysis generally exploits the fact that for a continuous random distribution it is assumed that $R_{ij}^3 x = \text{const}$, where R_{ij} denotes a typical distance between the ions. Implementation of this expression in a model for spin-glass freezing, given a known functional form for the radial dependence of the exchange interaction, then yields a theoretical prediction for $T_f(x)$ which can be compared with experimental data.

This procedure is elaborated in the Appendix for a continuous as well as a discrete distribution of ions. In the spirit of earlier analyses,[18,19] the spin-glass–freezing condition is based on the existence of a critical fraction of blocked or frozen ions at the freezing temperature. The fraction of these ions is determined by the probability of finding at least one ion within a sphere of radius $R_i(T)$, implicitly given by $J(R_i)S^2 = k_B T$. The results demonstrate the applicability of this approach also outside the limit of the very dilute regime to which it is usually restricted. Given a powerlike or exponential radial dependence of the interaction, the concentration dependence of T_f can be expressed as

$$\ln T_f \sim \frac{n}{3} \ln x \quad \text{for } J(R) = J_0 R^{-n}$$

or

$$\ln T_f \sim \alpha x^{-1/3} \quad \text{for } J(R) = J_0' \exp(-\alpha R) .$$

In Fig. 6 the experimental data $T_f(x)$ for $Zn_{1-x}Mn_xSe$ are plotted in the coordinates suitable for power and exponential dependence, respectively. A comparison between these shows that the simple power dependence $J(R) \sim R^{-n}$ seems to describe the data in the whole concentration range better than the exponential decay $[J(R) \sim e^{-\alpha R}]$. The exponent n deduced from Fig. 6 is $\simeq 6.8$. We would like to stress here that although it is clear that a power law yields a better fit to the experimental data than an exponential decay in the concentration range from far below to far above the percolation limit, one should not exclude the possibility that the x dependence of freezing temperature T_f can be different above and below the percolation limit. Therefore one should be careful in drawing definite conclusions from Fig. 6.

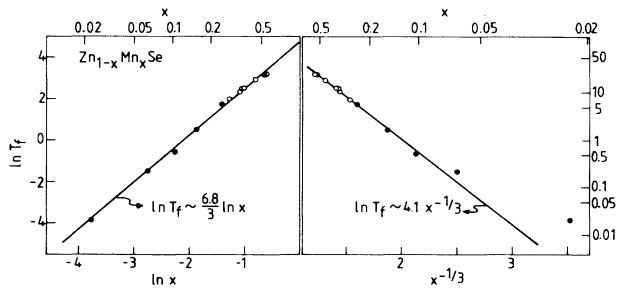

FIG. 6. Natural logarithm of the freezing temperature T_f as a function of (a) ln$x$ and (b) $x^{-1/3}$ for $Zn_{1-x}Mn_xSe$ (●, our data; ○, Ref. 12). The straight solid lines have slopes of (a) 2.3 and (b) −4.1.

B. Magnetic properties

It follows from the inspection of the experimental data and the analysis of the spin-glass transition that the Mn-Mn interaction in $Zn_{1-x}Mn_xSe$ is AF and that it is rather long ranged, decaying as $R^{-6.8}$. The relevant thermodynamic properties can be described with the so-called pair-approximation model, which is an approximative calculation method, particularly useful for random arrays with long-ranged interaction. It has been introduced by Matho[20] for canonical metallic SG's and was recently successfully used for DMS's as well.[2,3,9] This approximation is based on the assumption that the partition function of the system can be factorized into contributions of pairs of spins. We will consider two models in some detail: the extended nearest-neighbor pair approximation[2] (ENNPA) and the hierarchy pair approximation (HPA) of Rosso.[21] In the ENNPA each spin is considered to be coupled by an exchange interaction J_i only to its nearest magnetic neighbor, which may be located anywhere at a distance R_i from a reference site. The statistical weight of these pair configurations with various R_i (which can only take on discrete values depending on the symmetry of the host lattice) is assumed to be determined by the random distribution of the ions.

The Hamiltonian for a pair is given by

$$\mathcal{H}_i = -2J_i \mathbf{S}_i \cdot \mathbf{S}_j - g\mu_B (S_i^z + S_j^z) B^z , \tag{1}$$

where $J_i = J(R_i)$ and R_i denotes the distance between the sites i and j. If N_i is the number of lattice sites in a shell with radius R_i and using $n_i = \sum_{j=1}^{i} N_j$ for $j > 0$ and $n_0 = 0$, the probability for a pair formation can be taken as the probability of finding at least one nearest spin in the ith shell (assuming all $j < i$ shells empty) and reads for a random distribution as

$$\begin{aligned} P_i(x) &= (1-x)^{n_i - 1}[1-(1-x)^{N_i}] \\ &= (1-x)^{n_i - 1} - (1-x)^{n_i} . \end{aligned} \tag{2}$$

On the other hand, in the HPA the spins are arranged in a collection of separate pairs ordered by decreasing interactions.[21] The calculation of the probability distribution for pairs in this case is similar to that used in the ENNPA: $P_i(x)$ is a product of (a) the probability for a spin to have a magnetic neighbor at a distance R_i, and (b) the probability that both spins do not belong to a pair with a shorter R_i. We then obtain

$$P_i(x) = [1-(1-x)^{N_i}] \left[1 - \sum_{\substack{j=1 \\ (j \in R_i)}}^{n_i} P_j(x) \right]^2 , \tag{3}$$

where the summation runs over sites in the sphere R_i; some sites are skipped in the summation because the probabilities that ions i and j do not belong to a pair with shorter R_i are not independent.[21] The principal difference between the ENNPA and HPA is shown in Fig. 7 for a system of four ions. The calculated probability distributions for $x=0.023$ in both models are shown in Fig. 8. As could be expected, the number of pairs with small R_i ($i \leq 7$) is enhanced in the ENNPA, with respect to the HPA. This situation is reversed for more distant pairs. Since the probability distributions are known, the total partition function and other thermodynamic properties can be obtained by summing the respective pair contributions:

$$Z = \sum_{i=1}^{\infty} Z_i P_i(x)/2 \ , \tag{4}$$

$$C_m = \sum_{i=1}^{\infty} C_{mi} P_i(x)/2 \ . \tag{5}$$

Each pair contribution (Z_i, C_{mi}, and so on) contains the exchange parameter J_i. Following the results of the preceding section, we take $J_i = J_0/R_i^{6,8}$, where R_i is in units of the NN distance in the host lattice.

The summation over the shells i is carried up to shell $\bar{i}$ for which $\sum_{i=1}^{\bar{i}} P_i \geq 0.995$. For low concentrations ($x < 0.03$) usually $\bar{i} < 20$, being even less for higher concentrations.

The results of the specific-heat calculation for both the ENNPA and HPA are shown in Fig. 9 together with the experimental data. For J_0 (i.e., NN interaction) we have taken -13 K as indicated by high-field magnetization data.[22] Recent inelastic-neutron-scattering data[23] yielded a comparable value, although slightly lower. One can notice that at low temperatures ($T \leq 0.2$ K) the HPA gives larger values than the ENNPA, whereas for higher temperatures the situation is reversed. This results from the discussed difference in probability distributions (Fig. 8). The difference is much more significant for higher concentrations ($x \simeq 0.06$) than for lower ones ($x \simeq 0.01$), for which the ENNPA and HPA nearly coincide. It should be stressed that the specific-heat curves shown in Fig. 9 were simply calculated with no fitting to the experimental data. Presumably a better agreement will be obtained if J_i values are treated as adjustable parameters. Since the nearest-neighbor interaction J_0 is in-

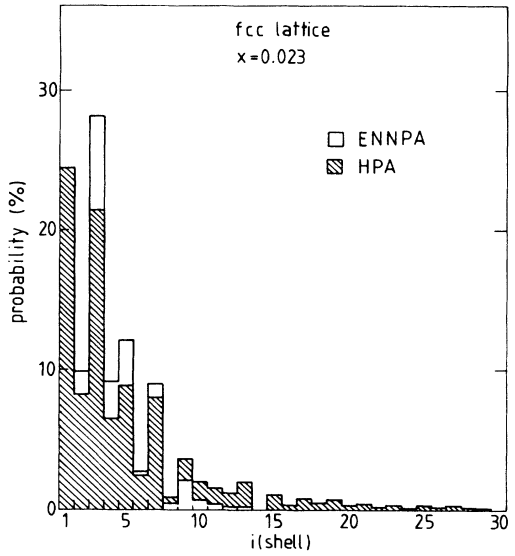

FIG. 8. Probability of finding at least one magnetic neighbor in shell i represented by the blank histogram [Eq. (2)], and probability for a spin to have at least one magnetic neighbor in shell i under the condition that both spins do not belong to a pair with a shorter distance [Eq. (3)] represented by the shaded histogram.

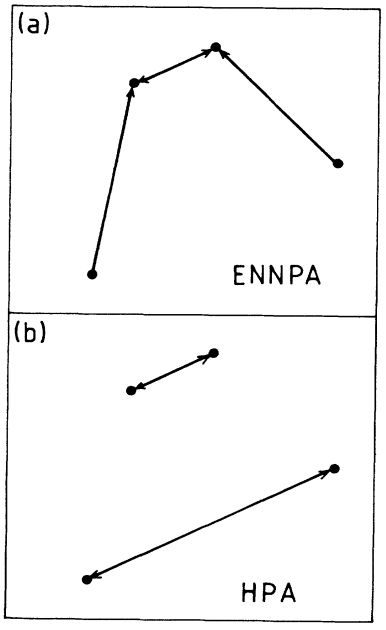

FIG. 7. Pair formation in the (a) ENNPA and (b) HPA. The arrows represent spin-spin interactions.

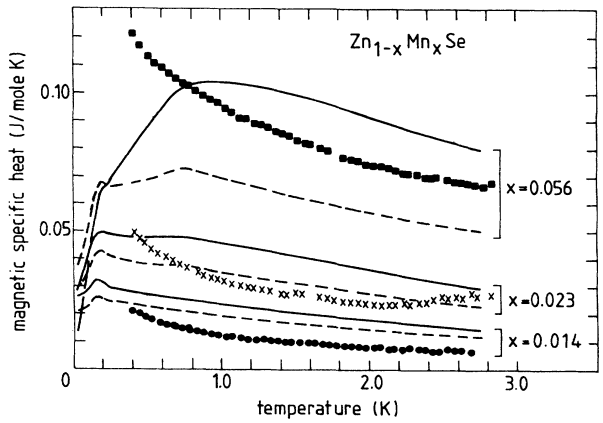

FIG. 9. Zero-field magnetic specific heat calculated in the ENNPA (solid lines) and HPA (dashed lines) together with experimental data.

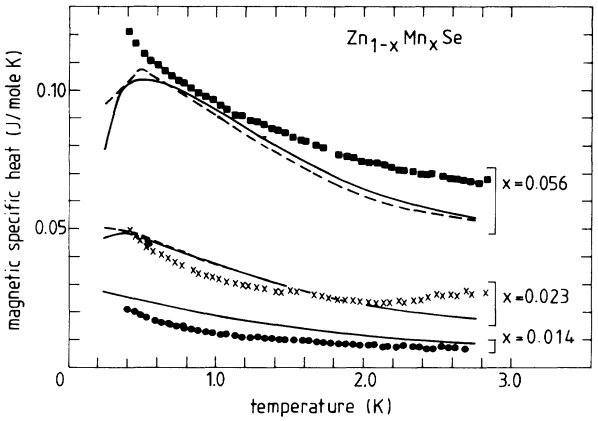

FIG. 10. Magnetic specific heat of $Zn_{1-x}Mn_xSe$. The dashed lines represent calculations with the ENNPA as described in the text using $J_0/k_B=-13$ K and $J_i/k_B=-7/R^{6.8}$ K. The solid lines represent the ENNPA with triples included.

ferred from independent experiments and the radial dependence from $T_f(x)$, we inserted J_0 as a constant value ($=-13$ K) and assumed for further neighbors that $J_i=J_1/R_i^{6.8}$ ($i>0$), where J_1 is the only adjustable parameter. J_1 was chosen to obtain the best overall agreement for all three experimental quantities: C_m, M, and χ. For the final calculations we have extended our ENNPA in a similar way as for $(CdMn)_3As_2$ (Ref. 2) and $(ZnMn)_3As_2$ (Ref. 3); we considered not only pairs but also "triples" (i.e., configurations in which two spins are located at the same distance from the reference site).

The results of ENNPA calculations with $J_0=-13$ K and $J_1=-7$ K are shown in Figs. 5 and 10 (C_m), 11 (M), and 12 (M). The high-temperature susceptibility calculations for $Zn_{0.95}Mn_{0.05}Se$ yield a Curie-Weiss temperature $\Theta=-45$ K which is in perfect agreement with the experiment.[12] The high-field magnetization, shown in Fig.

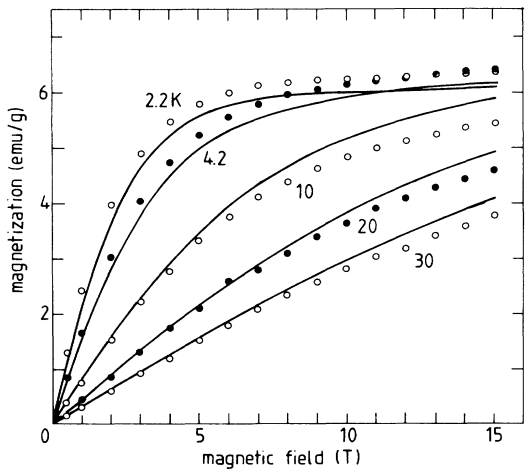

FIG. 11. High-field magnetization of $Zn_{0.95}Mn_{0.05}Se$. The solid lines represent calculations with the ENNPA using $J_0/k_B=-13$ K and $J_i/k_B=-7/R^{6.8}$ K.

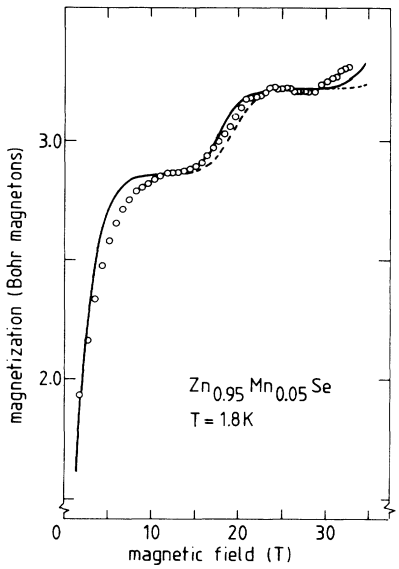

FIG. 12. Steplike magnetization of $Zn_{0.95}Mn_{0.05}Se$ (Ref. 24) together with the ENNPA prediction (solid line, $J_0/k_B=-12$ K and $J_i/k_B=-7/R^{6.8}$ K, dashed line, $J_0/k_B=-13$ K and $J_i/k_B=-7/R^{6.8}$ K). Since no absolute value of magnetization is given in Ref. 24 the magnetization was scaled at 25 T.

12, has been recently fitted with a model including a nearest-neighbor interaction $J_0=-9.9$ K and a mean field.[24] Our results also show that a satisfactory description can be obtained with the same set of parameters as used for the other thermodynamic quantities.

The ENNPA may be further extended by combining it with a mean-field approximation to account for the average interaction of a spin with the other spins not belonging to a pair (i.e., spins with $i>\bar{i}$). The results generally confirm this conjecture, although the obtained correction is rather small. We conclude that, although these extensions do not significantly improve the results and some systematic deviations remain, the general agreement shows that it is, in principle, possible to explain the behavior of specific heat, magnetization, and susceptibility simultaneously, without the need to adjust the random distribution of the Mn ions. As we quoted before, some C_m data on $Zn_{1-x}Mn_xSe$ with a nominal Mn concentration of $x=0.01$ were recently published by Keesom.[16] Assuming only contributions from singles, pairs, and triples he was able to describe the data rather well. However, since essentially both the total Mn concentration as well as the statistical distribution were used as a fitting parameter, a comparison with these results does not seem very significant.

IV. DISCUSSION

The analysis of the concentration dependence of the freezing temperature, as performed for $Zn_{1-x}Mn_xSe$ in the preceding section, can also be applied to other DMS's. The available data on $T_f(x)$ for a number of them are gathered in Fig. 13. In all cases it appears that a description of $T_f(x)$ based on a power-law dependence

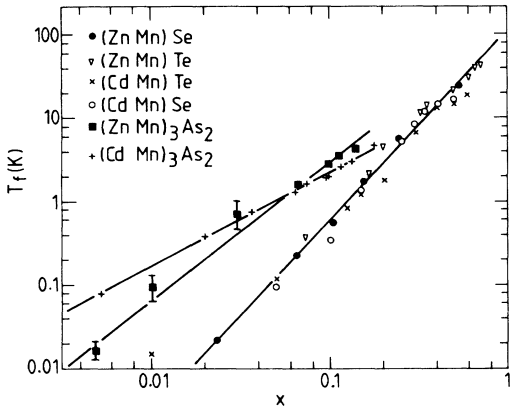

FIG. 13. Freezing temperature T_f as a function of the Mn concentration x for various DMS's on logarithmic scale. The straight lines are fitted to the data yielding the power dependence $J(R)\sim R^{-n}$ as tabulated in Table II. References on the origin of the data are given in the text.

of $J(R)=J_0R^{-n}$ fits the data in the whole concentration range rather well, in contrast to the description based on an exponential decay of $J(R)$. Whether this is indicative of a specific mechanism remains to be seen, however, since (as was argued before[8]) it is not *a priori* clear whether the same mechanism is responsible for the spin-glass freezing below and above the percolation limit.

The exponents n deduced from Fig. 13 are tabulated in Table II. The various systems in Table II are arranged in order of decreasing gap. Reviewing the table gives rise to the following comments. The considerable increase of the range ($\sim 1/n$) of the interaction going from wide-band-gap materials to small-band-gap materials is obvious. This fact is not inconsistent with the expectations based on the Bloembergen-Rowland exchange interaction[25] as the driving mechanism behind the spin-glass freezing. In this case, however, an exponential decrease [$J(R)\sim e^{-\alpha R}$] should have been expected and the apparent universal range of the exchange for the II-VI compounds, irrespective of the appreciable variation of the gap magnitude, is somewhat surprising. Moreover, if superexchange was the driving mechanism, as suggested by Larson *et al.*,[26] at least for the nearest-neighbor interactions, an increasing range of the interaction would be related to an increasing covalent character of the bonding.[26] Roughly speaking, such an increasing covalence may indeed by expected when the II-VI systems are compared with II-V and IV-VI systems. More detailed information can be obtained from the location of the energy of the Mn d levels with respect to the top of the valence band. Recently Taniguchi *et al.*[27] obtained information about the Mn $3d$ density of states and p-d hybridization in the series $Cd_{1-x}Mn_xY$ (Y=S, Se, and Te). They concluded that for this series the degree of p-d hybridization increases upon going from Te to S. However, the data tabulated in Table II do not reflect the expected systematic change in range of the interaction.

In fact, a most remarkable feature of the data on T_f versus x as shown in Fig. 13 is the surprising universal behavior of the II-VI wide-band-gap materials. Not only is the concentration dependence analogous (and thus the range $1/n$), but the absolute magnitude of the freezing temperature is also the same, taking into account the scattering of the data. In view of the fact that considerable differences exist between the lattice parameters of the II-VI compounds in this series (up to 20%), a variation of the freezing temperature by a factor of 2 or 3 might have been anticipated within the concept of our model, given the pronounced radial dependence of the interaction strength $J(R)$. The data apparently do not support this conjecture. This might be considered an indication that, besides the interaction strength, the freezing process is also determined by topological criteria.

As we quoted in the Introduction, the overall characteristics of DMS's, include, among others, AF long-ranged interactions and spin-glass formation for a wide range of concentrations. It has been questioned whether real spin-glass formation is possible in a random diluted array coupled by long-range isotropic AF interactions only, since in that case the driving mechanisms of frustration or competition would not be effective.[17] To start with, we would like to emphasize that the present exper-

TABLE II. Type, concentration range, band gap, nearest-neighbor distance, and exponent n of various DMS's.

Material	Type	x range	E_g (eV)	NN distance (Å) (for $x=0$)	n	Ref.
$Zn_{1-x}Mn_xS$	II-VI	0.3–0.4	$\simeq$3.8	3.83	$\simeq$6.8	31
$Zn_{1-x}Mn_xSe$	II-VI	0.02–0.5	2.8–3	4.00	6.8	This paper, 12
$Zn_{1-x}Mn_xTe$	II-VI	0.07–0.6	2.4–2.8	4.31	6.8	8, 32
$Cd_{1-x}Mn_xSe$	II-VI	0.05–0.5	1.8–2.6	4.28	$\simeq$6.8	7, 30
$Cd_{1-x}Mn_xTe$	II-VI	0.01–0.6	1.6–2.5	4.58	$\simeq$6.8	4, 19, 6, 33
$Hg_{1-x}Mn_xTe$	II-VI	0.02–0.5	$\simeq$0–1.1	4.55	$\simeq$5	5,34,35
$Hg_{1-x}Mn_xSe$	II-VI	0.02–0.3	$\simeq$0	4.30	$\simeq$5.0	37
$(Zn_{1-x}Mn_x)_3As_2$	II-V	0.005–0.1	$\simeq$1	2.94	4.5	3
$(Cd_{1-x}Mn_x)_3As_2$	II-V	0.005–0.2	0–0.2	3.17	3.5	2
$Pb_{1-x}Mn_xTe$	IV-VI	0.03–0.1	0.2–0.4	4.56	3	36

iments on $Zn_{1-x}Mn_xSe$ did yield the observation of typical spin-glass characteristics. These include the cusp in the susceptibility, a continuous specific heat, and a difference in zero-field-cooled and field-cooled magnetizations, both for concentrations above as well as below the percolation limit. We feel that with these data the canonical spin-glass nature of the transition is strongly supported.[17]

With respect to the fundamental question about the spin-glass freezing in DMS's as such, we would like to point out that the anisotropy might play an important role. From Monte Carlo calculations and renormalization-group treatments,[28,29] it has been suggested that, in general, an additional anisotropy in an isotropic system will lower the critical dimension and a small anisotropy is needed to activate a clearcut transition. More specifically, it was suggested for impurity spins in III-V semiconductors that the random anisotropy of the indirect exchange is the driving force towards a spin-glass state, irrespective of the sign of the exchange integral.[38]

Experimental evidence of such an additional anisotropy in DMS's is scarce, however, though not completely absent. For the present compound $Zn_{1-x}Mn_xSe$, electron-spin-resonance results were reported for dilute samples, indicating a uniaxial single-ion anisotropy $D=0.1$ K.[39] Moreover, inspection of the specific-heat data as shown in Fig. 4 indicates an increase in C_m at the lowest temperatures, which is not reflected in the calculations. This is by no means unique for $Zn_{1-x}Mn_xSe$ and has been observed in a number of DMS's. Earlier attempts have been made in $Cd_{1-x}Mn_xSe$ to explain this behavior in terms of a single-ion anisotropy, although in that case no single-ion splitting was observed in ESR experiments.[30] For $Zn_{1-x}Mn_xSe$, the reported value of $D\sim 0.1$ K can, as calculations of the resulting Schottky anomaly have shown, explain, in principle, the increase of the low-temperature C_m. Further direct evidence on this anisotropy is, however, difficult to obtain. Preliminary experiments on a single crystal with 1 at. % Mn^{2+} in an external field applied along the principal axis showed no macroscopic preferred direction. This, however, can be understood by assuming random local axes, in agreement with the ESR results.[39] In order to establish the presence of these anisotropic terms and their influence on the freezing process, further research is necessary.

ACKNOWLEDGMENTS

It is a pleasure to thank C. v. d. Steen, H. J. M. Heyligers, T. F. H. v. d. Wetering, E. P. V. Maesen, J. Flokstra, T. v. d. Pasch, and J. Zeegers for the experimental and numerical assistance. The authors also wish to acknowledge stimulating discussions with Professor R. R. Galazka, Professor J. A. Mydosh, Professor J. K. Furdyna and Dr. R. Stepniewski. Professor J. K. Furdyna is also acknowledged for making susceptibility data available to us prior to publication. One of us (A.T.) wishes to express his gratitude for the hospitality during his stay at the Eindhoven University of Technology.

APPENDIX

In this appendix we present a simple model which corroborates the usefulness of the scaling analysis relating the freezing temperature to the concentration. This model is based generally on the idea of Smith[18] and Escorne *et al.*,[19] defining the SG freezing as the process of cluster blocking.

We consider a particular magnetic ion which may be blocked (frozen) by coupling with its magnetic neighbors if the exchange energy $J(R)S^2$ is larger than the thermal energy k_BT. On the other hand, an ion is considered to be "free" (i.e., freely responding to the external magnetic field) if it has no magnetic neighbor inside the sphere of radius R_i defined by

$$J(R_i)S^2=k_BT\ . \tag{A1}$$

The probability that a particular ion is free is given by

$$P_{\text{free}}=(1-x)^{n_i}\ , \tag{A2}$$

where n_i is the total number of lattice sites inside a sphere with volume $\frac{4}{3}\pi R_i^3$.

Equation (A1) relates R_i to the temperature and P_{free} may be calculated directly for a particular lattice, as we will show below. Before that we consider the approxi-

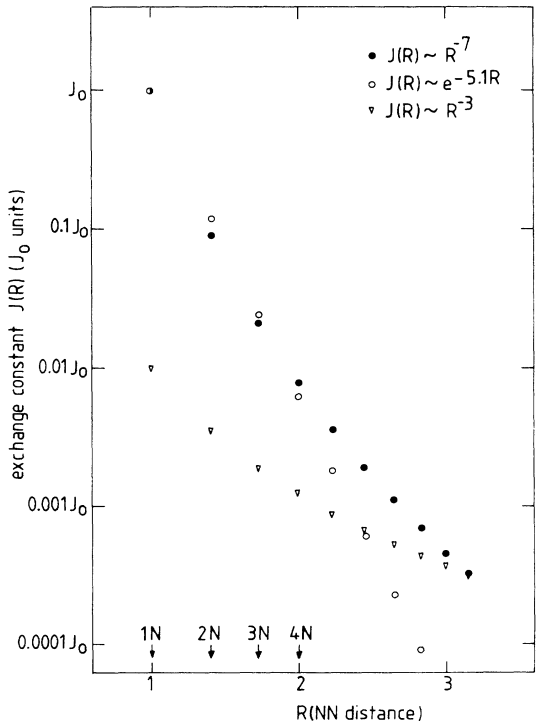

FIG. 14. Exchange constant $J(R)$ and radial dependence for $J(R)\sim R^{-7}$ (●) and $J(R)\sim e^{-5.1R}$ (○). The prefactors are chosen so that $J(R_{NN})=J_0$. Arrows indicate nearest neighbors (1N), next nearest neighbors (2N), and so on. For comparison, $J(R)\sim R^{-3}$, corresponding to dipole-dipole interaction, is also shown. The prefactor for this case was chosen to be $0.01J_0$, an overestimation of the dipole-dipole interaction in DMS's.

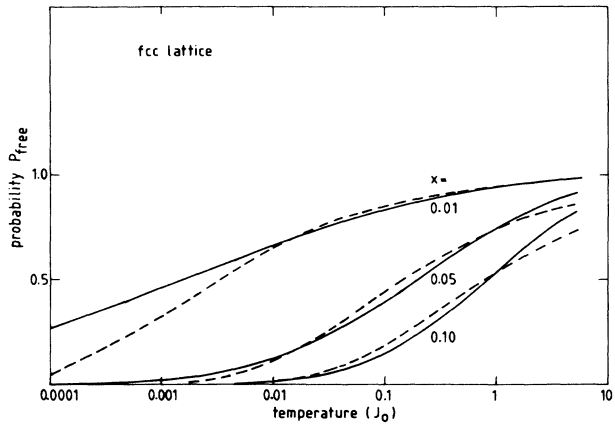

FIG. 15. Probability that a magnetic ion in a fcc lattice is not blocked for $x=0.01$, 0.05, and 0.10 as a function of temperature for continuous distributions. Solid line, $J(R)\sim e^{-5.1R}$ (A5b)]; dashed line, $J(R)\sim R^{-7}$ [(A5a)]. Temperature is in J_0 units, where J_0 is the interaction value for the nearest neighbors.

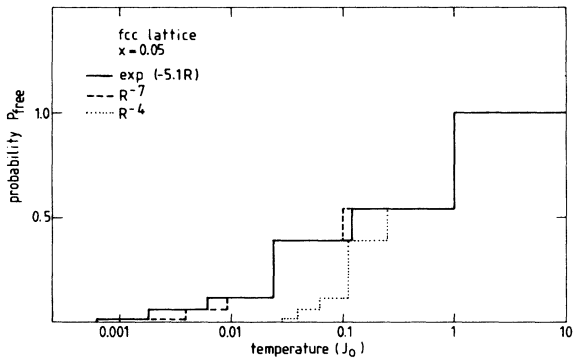

FIG. 16. Probability that a magnetic ion in a fcc lattice is not blocked as a function of temperature for $x=0.05$. Solid line, $J(R)\sim e^{-5.1R}$; dashed line, $J(R)\sim R^{-7}$; dotted line, $J(R)\sim R^{-4}$. All interactions are chosen so that all have the same value (J_0) at nearest-neighbor distance.

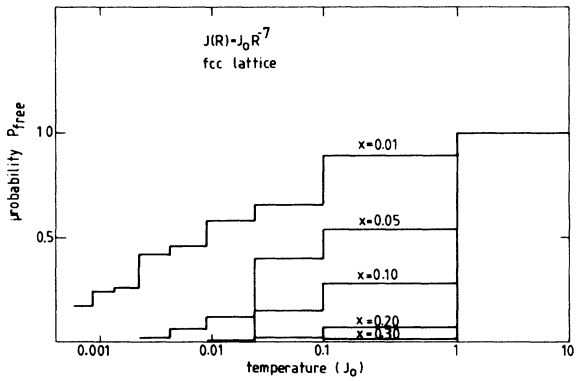

FIG. 17. Probability that a magnetic ion in a fcc lattice is not blocked as a function of temperature for $J(R)\sim R^{-7}$ and $x=0.01$, 0.05, 0.10, 0.20, and 0.30. At the nearest-neighbor distance $J(R)=J_0$.

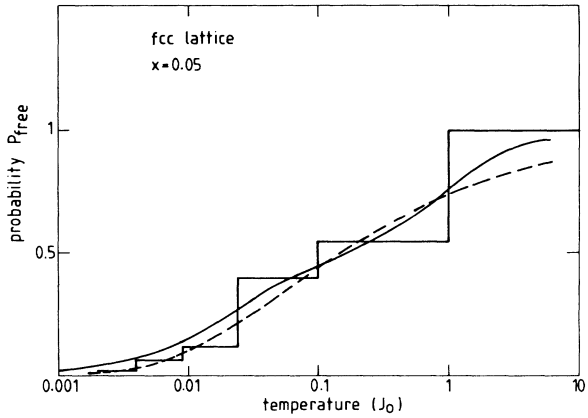

FIG. 18. Probability that a magnetic ion in a fcc lattice is not blocked for $x=0.05$ and $J(R)\sim R^{-7}$. Solid steplike line, distribution the same as in Fig. 17; solid line, the same distribution but convoluted with exponential function with $\gamma=0.4J_0$; dashed line, continuous approximation [Eqs. (A5) and (A6)].

mation for a very dilute system which results in analytical solution. For a very dilute system (i.e., semicontinuous distribution of ions) we have

$$n_i=\tfrac{4}{3}\pi R_i^3/A\ , \tag{A3}$$

where A is volume per one lattice site ($A=a^3$ for simple-cubic structure and $A=\frac{1}{4}a^3$ for fcc structure).

For DMS materials the exchange constant is supposed to be relatively long ranged (i.e., extending also for further, not only the nearest, neighbors) and depending on distance as

$$J(R)=J_0R^{-n} \tag{A4a}$$

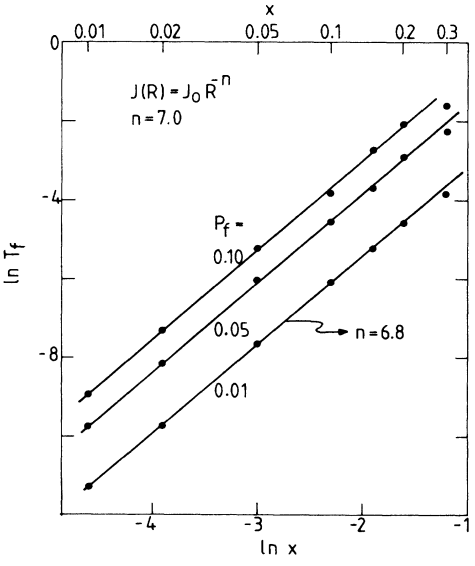

FIG. 19. Logarithm of the freezing temperature resulting from probability distribution (as discussed in the text) as a function of logarithm of concentration for $J(R)=J_0R^{-n}$, $n=7$, for different freezing probabilities $P_f=0.01$, 0.05, and 0.10. The slope of the lines yields an exponent $n=6.8$.

TABLE III. Freezing temperatures T_f (in units of J_0S^2) for various P_f values and concentrations.

$J(R)$	P_{free}	Concentration 0.01	0.02	0.05	0.10	0.15	0.20	0.30
	0.10	3.77×10^{-6}	1.39×10^{-4}	4.62×10^{-3}	2.45×10^{-2}	0.0773	0.139	0.208
$e^{-5.1R}$	0.05	8.11×10^{-7}	3.49×10^{-5}	1.58×10^{-3}	1.19×10^{-2}	0.0284	0.0619	0.105
	0.01	3.94×10^{-8}	2.69×10^{-6}	1.95×10^{-4}	2.18×10^{-3}	0.00615	0.119	0.0228
	0.10	1.31×10^{-4}	6.55×10^{-4}	5.41×10^{-3}	0.0218	0.0657	0.127	0.205
$1/R^7$	0.05	5.82×10^{-5}	2.90×10^{-4}	2.38×10^{-3}	0.0106	0.0249	0.0549	0.103
	0.01	1.25×10^{-5}	5.90×10^{-5}	4.88×10^{-4}	0.00225	0.00542	0.0105	0.0221

or

$$J(R)=J_0'e^{-\alpha R}\ . \tag{A4b}$$

In Fig. 14 both relations (A4a) and (A5b) are shown for $n=7$ and $\alpha=5.1$ as proposed for wide-band-gap DMS's.[8,9] Finally, we get, from (A1)–(A4),

$$P_{\text{free}}=(1-x)^{(4\pi/3)(J_0S^2/T)^{3/n}}\ , \tag{A5a}$$

$$P_{\text{free}}=(1-x)^{(4\pi/3)[1/\alpha\ln(J_0'S^2/T)]^3}\ . \tag{A5b}$$

The obtained distributions are shown in Fig. 15 for a fcc lattice, showing a gradual decrease of the probability that an ion is not frozen with decreasing temperature. We assume that for a sufficiently small $P_{\text{free}}=P_f$, where P_f is an arbitrarily chosen constant depending on the specific mechanism, the ion system may be considered frozen, the temperature at which P_f is reached defined as the freezing temperature T_f [$P_{\text{free}}(T_f)=P_f$]. Then, from (A5), one may obtain the following scaling laws:

$$\ln T_f\sim\frac{n}{3}\ln x \quad \text{for (A4a)}\ , \tag{A6a}$$

$$\ln T_f\sim\alpha x^{-1/3} \quad \text{for (A4b)}\ . \tag{A6b}$$

These relations have also been reported by other authors[18] and are applied in this article.

We now abandon the limitation to the very dilute case (continuous distribution assumption) and extend our model to higher x. In Fig. 16 the probability distribution versus temperature is shown for $x=0.05$ for both interactions (A4a) and (A4b). As can be noticed, there is only a slight difference between the power (A4a) and exponential decay (A4b), since for $T\geq0.003J_0$ (and $\alpha=5.1$, $n=7$) both dependencies are practically the same (cf. Fig. 14). It is also evident that for a longer-range interaction (such as R^{-4}) the ion system freezes faster at higher temperatures than for a shorter-range interaction (such as R^{-7}). The steplike structure of the P_{free} distribution is a consequence of the "sharp" freezing condition (A1). The steps correspond to the passing through consecutive discrete coordination spheres. In Fig. 17 the P_{free} distributions are shown for $0.01\leq x\leq0.30$. It follows from this figure that for low concentrations ($x\leq0.05$) the ion system freezes gradually, whereas for higher x ($x>0.10$) rather abrupt freezing may be observed. For $x>0.3$ (i.e., exceeding the validity of our model) the P_{free} distribution practically does not depend on x, as could be expected. To obtain a more realistic model we may "smooth" the freezing condition (A1) by convoluting the obtained distributions with a Gaussian, Lorentz, or exponential function. The result for an exponential function [$\frac{1}{2}\exp(-|\log_{10}T|/\gamma)$, where γ is the full width at half maximum parameter], is shown in Fig. 18 for $x=0.05$ and arbitrarily chosen as $\gamma=0.4J_0$. Freezing temperatures T_f found from this convoluted distributions are tabulated in Table III for various P_f values. It may be noticed that the T_f values obtained for $P_f=0.05$ are well comparable with experimental results for $Zn_{1-x}Mn_xSe$ ($J_0=-13$ K and $S=\frac{5}{2}$). They also obey formulas (A6) quite well. An example is shown in Fig. 19 for $J(R)=J_0R^{-7}$ for $P_f=0.10$, 0.05, and 0.01. Good linearity may be observed for $x\leq0.20$. The n value deduced from the slope is $\simeq6.8$, which compares favorably with the inserted value $n=7$. We therefore feel confident in using scaling laws in the form (A6) to describe our data, even for a discrete lattice and at somewhat higher concentrations.

*On leave from the Institute of Experimental Physics, The University of Warsaw, Hoża 69, PL-00-681 Warsaw, Poland.

[1]See the following review papers: N. B. Brandt and V. V. Moshchalkov, Adv. Phys. **33**, 193 (1984); J. K. Furdyna, J. Appl. Phys. **53**, 8637 (1982); J. A. Gaj, J. Phys. Soc. Jpn. Suppl. **49**, A797 (1980).

[2]C. J. M. Denissen, H. Nishihara, J. C. van Gool, and W. J. M. de Jonge, Phys. Rev. B **33**, 7637 (1986); W. J. M. de Jonge, M. Otto, C. J. M. Denissen, F. A. P. Blom, C. v. d. Steen, and K. Kopinga, J. Magn. Magn. Mater. **31-34**, 1373 (1983).

[3]C. J. M. Denissen *et al.*, Phys. Rev. B **36**, 5316 (1987).

[4]R. R. Gałązka, S. Nagata, and P. H. Keesom, Phys. Rev. B **22**, 3344 (1980).

[5]S. Nagata, R. R. Gałązka, D. P. Mullin, H. Arbarzadeh, G. D. Khattak, J. K. Furdyna, and P. H. Keesom, Phys. Rev. B **22**, 3331 (1980).

[6]M. A. Novak, O. G. Symko, D. J. Zheng, and S. Oseroff, J. Appl. Phys. **57**, 3418 (1985).

[7]M. A. Novak, O. G. Symko, D. G. Zheng, and S. Oseroff, Physica **126B** 469 (1984).

[8]A. Twardowski, C. J. M. Denissen, W. J. M. de Jonge, A. T. A. M. de Waele, M. Demianiuk, and R. Triboulet, Solid State Commun. **59**, 199 (1986).

[9]C. J. M. Denissen and W. J. M. de Jonge, Solid State Commun. **59**, 503 (1986).

[10]W. J. M. de Jonge, A. Twardowski, and C. J. M. Denissen, in *Diluted Magnetic (Semimagnetic) Semiconductors,* Material Research Society Symposium Proceedings No. 89, edited by S. von Molar, R. L. Aggarwal, and J. K. Furdyna (unpublished).

[11]A. Twardowski, M. von Ortenberg, M. Demianiuk, and R. Pauthenet, Solid State Commun. **51**, 849 (1984).

[12]J. K. Furdyna (private communication).

[13]E. Michalski, M. Demianiuk, S. Kaczmarek, and J. Zmija, Electron Technol. **13**, 4, 9 (1982).

[14]A. Twardowski, T. Dietl, and M. Demianiuk, Solid State Commun. **48**, 345 (1983).

[15]R. B. Bylsma, W. M. Becker, J. Kossut, and U. Debska, Phys. Rev. B **33**, 8207 (1986).

[16]P. H. Keesom, Phys. Rev. B **33**, 6512 (1986).

[17]J. A. Mydosh, in *Hyperfine Interactions,* Vol. 31 of *Lecture Notes in Physics* (Springer, New York, 1986), p. 347.

[18]D. A. Smith, J. Phys. F **5**, 2148 (1975).

[19]M. Escorne, A. Mauger, R. Triboulet, and J. L. Tholence, Physica **107B**, 309 (1981).

[20]K. Matho, J. Low Temp. Phys. **35**, 165 (1979).

[21]M. Rosso, Phys. Rev. Lett. **44**, 1541 (1980); P. A. Thomas and M. Rosso, Phys. Rev. B **34**, 7936 (1986).

[22]Y. Shapira, S. Foner, D. H. Ridgley, K. Dwight, and A. Wold, Phys. Rev. B **30**, 4021 (1984).

[23]T. M. Giebultowicz, J. J. Rhyne, and J. K. Furdyna, Proceedings of the Thirty-First Annual Conference on Magnetism and Magnetic Materials, Baltimore, 1986, edited by N. C. Coon, J. D. Adam, J. A. Beardsley, and D. L. Huber [J. Appl. Phys. **61**, 3537 (1987); **61**, 3540 (1987)].

[24]J. P. Lascaray, M. Nawrocki, J. M. Broto, and M. Rakoto, and M. Demianiuk, Solid State Commun. **61**, 401 (1987).

[25]N. Bloembergen and T. J. Rowland, Phys. Rev. **97**, 1679 (1955); G. Bastard and C. Lewiner, *ibid.* **20**, 4256 (1979).

[26]W. Geertsma. C. Hass, G. A. Sawatzky, and G. Vertogen, Physica **86-88A**, 1039 (1977); G. A. Sawatzky, W. Geertsma, and C. Hass, J. Magn. Magn. Mater. **3**, 37 (1976); B. E. Larson, K. C. Hass, H. Ehrenreich, and A. E. Carlsson, Solid State Commun. **56**, 347 (1985).

[27]M. Taniguhi, M. Fujimori, M. Fujisawa, T. Mori, I. Souma, and Y. Oka, Solid State Commun. **62**, 431 (1987).

[28]A. J. Bray, M. A. Moore, and A. P. Young, Phys. Rev. Lett. **56**, 2641 (1986).

[29]A. Chakrabarti and Ch. Dasgupta, Phys. Rev. Lett. **56**, 1404 (1986).

[30]C. D. Amarasekara, R. R. Gałązka, Y. Q. Yang, and P. H. Keesom, Phys. Rev. B **27**, 2868 (1983).

[31]Y. Q. Yang, P. H. Keesom, J. K. Furdyna, and W. Giriat, J. Solid State Chem. **49**, 20 (1983).

[32]S. P. McAlister, J. K. Furdyna, and W. Giriat, Phys. Rev. B **29**, 1310 (1984).

[33]M. Escorne and A. Mauger, Phys. Rev. B **25**, 4674 (1982).

[34]N. B. Brandt, V. V. Moshchalkov, A. O. Orlov, L. Skrbek, I. M. Tsidil'kovskii, and S. M. Chudinov, Zh. Eksp. Teor. Fiz. **84**, 1050 (1983) [Sov. Phys.—JETP **57**, 614 (1983)].

[35]A. Mycielski, C. Rigaux, M. Menaut, T. Deitl, and M. Otto, Solid State Commun. **50**, 257 (1984).

[36]M. Escorne, A. Mauger, J. L. Tholence, and R. Triboulet, Phys. Rev. B **29**, 6306 (1984).

[37]R. R. Gałązka, W. J. M. de Jonge, and A. T. A. M. de Waele (unpublished).

[38]N. P. Il'in and I. Ya. Korenblit, Zh. Eksp. Teor. Fiz **81**, 2070 (1981) [Sov. Phys.—JETP **54**, 1100 (1982)].

[39]J. Kreissl and W. Gehlhoff, Phys. Status Solidi A **81**, 701 (1984).